analytical chemistry

pubs.acs.org/ac Article

Web-Based Open-Source Tool for Isotachophoresis

Alexandre S. Avaro, Yixiao Sun, Kaiying Jiang, Supreet S. Bahga, and Juan G. Santiago*

Cite This: *Anal. Chem.* 2021, 93, 15768−15774 Read Online

ACCESS | Metrics & More | Article Recommendations | Supporting Information

ABSTRACT: We present the development of a client-side web-based simulator for complex electrophoresis phenomena, including isotachophoresis. The simulation tool is called Client-based Application for Fast Electrophoresis Simulation (CAFES). CAFES uses the broad cross-browser compatibility of JavaScript to provide a rapid and easy-to-use tool for coupled unsteady electromigration, diffusion, and equilibrium electrolyte reactions among multiple weak electrolytes. The code uses a stationary grid (for simplicity) and an adaptive time step to provide reliable estimates of ion concentration dynamics (including pH profile evolution), requiring no prior installation nor compilation. CAFES also offers a large database of commonly used species and their relevant physicochemical properties. We present a validation of predictions from CAFES by comparing them to experimental data of peak- and plateau-mode isotachophoresis experiments. The code yields accurate estimates of interface velocity, plateau length and relative intensity, and pH variations while significantly reducing the computation time compared to existing codes. The tool is open-source and available for free at https://microfluidics.stanford.edu/cafes.

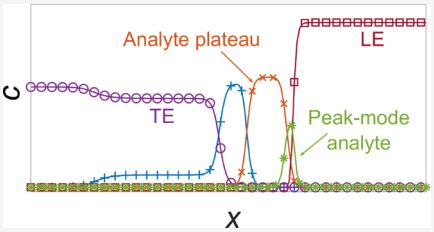

INTRODUCTION

Isotachophoresis (ITP) is a well-established electrophoresis technique for preconcentration, separation, and purification of ionic sample species depending on their effective electrophoretic mobility. ITP uses a leading electrolyte (LE) buffer and trailing electrolyte (TE) buffer. Sample ions focus if their mobility magnitude is larger than the TE's co-ion and smaller than the LE's co-ion. Trace ions focused for a short time will focus at the LE-to-TE interface in relatively narrow, strongly overlapping peaks.[1,2] A higher concentration sample ion focused for longer times can eventually develop its own purified zone called a plateau. These plateaus have a maximum concentration determined by their absolute mobility, acid dissociation constant, and the properties of the LE buffer. Multiple sample ions can be focused and separated into a train of adjoining plateaus between the LE and TE.[2,3] Interest in ITP is growing due to its versatility, robustness, and ease of integration into microfluidic assay systems. For example, ITP can purify nucleic acids from complex samples,[4] be integrated with capillary electrophoresis to achieve both high sensitivity and resolution[5] and can be used to control and accelerate biochemical reactions.[6] ITP can be integrated into one or more steps of complex assays such as immunoassays[7] or CRISPR-based enzyme detection.[8]

Easily accessible simulation tools offer an excellent way to understand the basics of ITP, design, and model ITP processes and to help troubleshoot and understand complex ITP phenomena. One example design challenge is the selection and specification of buffer ions, in particular, the initial concentrations and mobilities of LE co-ion, TE co-ion, and the LE counter-ion. Also interesting is the evaluation of various sample injection and other spatial configuration strategies. Several ITP simulation packages, namely numerical solvers for coupled, unsteady, multispecies electromigration and diffusion, are currently available. Among these, the most useful and robust for quick evaluation of buffer chemistries, injection schemes, and ITP dynamics are tools that consider the highly simplified case of unsteady but one-dimensional transport, including multi-species electromigration and diffusion of weak electrolytes. The original version of SIMUL,[9] whose latest version was published in 2021,[10] was likely the earliest of such freely available, nonlinear electrophoresis tools. The current version of SIMUL can, among other features, be used to optimize separation conditions, analyze focusing and preconcentration of several analytes, and capture electromigration dispersion. SPRESSO[11] is an open-source and free tool first developed in 2009, which includes a sixth-order compact finite difference scheme, an adaptive grid refinement to resolve high gradients, moving frames of reference for faster simulations, and a detailed model for dependence of mobility and dissociation constants. Bahga et al.[12] added the ability to account for ionic strength effects on both pK_a of ions and ion mobilities. More recently, Bercovici[13] published a package based on SPRESSO that included a new module for handling finite kinetic rate reactions among sample ions. All of these tools require some preparation by the user prior to execution, including download, file extraction, and operating system-dependent installation. The improved accuracy and

Received: September 9, 2021
Accepted: November 2, 2021
Published: November 17, 2021

complexity of these codes also mean that their execution is resource-intensive in terms of computational time and computer hardware requirements. Consequently, these simulators do not offer a short turn-around time for setting up and performing ITP simulations. Moreover, none of these simulators can be used on low-power devices such as tablets and smartphones, which have found increasing utility in laboratory and classroom settings.

Most ITP process designs require only one-dimensional models as these require the least computational expertise on the part of the user and provide the fastest simulations. Short simulation times enable rapid evaluation of candidate buffer ions and injection strategies. The main quantities of interest in such designs are the general "where and when" of the various species and the spatiotemporal development of pH. The latter is important as it governs weak electrolyte mobility as well as, for example, the stability, activity, and solubility of biochemical species. The "where and when" includes the time for plateaus and/or peaks to develop, the rate of accumulation of species and the net amount of substance(s) accumulated in these zones, the velocities of interfaces and peaks, the spatial order of plateaus, and estimates of the concentration of peaks and plateaus at the place and time of detection or elution. With the exception of peak-mode concentration, all of the latter quantities are weak functions of the spatial extent of the thin high-gradient regions between plateaus. These regions are, ideally, governed by the competing effects of nonuniform electromigration and diffusion. In practice, the spatial extent of such interfaces also depends on the dispersive effects associated with two- and three-dimensional geometries, externally applied pressure gradients, and internally generated pressure-driven flows (e.g., from residual electroosmotic flow or Joule heating).[14] The latter effects are difficult to capture and validate experimentally, and so it is fortunate that the precise prediction of the spatial profile of such interfaces is not a requirement for most ITP assays.[11,14] Even the advanced electrophoresis simulators such as SIMUL and SPRESSO do not model these practically observed dispersive effects, reducing the need for resolving steep concentration gradients using computationally expensive simulations.

In view of these considerations, we here present a simple-to-use ITP simulation tool we have called Client-based Application for Fast Electrophoresis Simulation (CAFES). CAFES is a free and open-source simulation of ITP, which benefits from the client-side features and wide cross-browser compatibility of JavaScript. CAFES can be used for simulating ITP processes through various web browsers on devices running any operating system, including mobile devices. The code enables accurate and fast evaluation of pH and the "when and where" of species in ITP with the relatively minor trade-off of offering only an approximate evaluation of the spatial extent of the highest gradients in an ITP process (e.g., the width of a highly focused peak or the details of the interface between adjoining plateaus). CAFES offers an intuitive interface, enabling the specification of a wide range of buffer species and sample injection configurations and mixtures. It includes a database[11,15] of 521 selectable species in addition to custom user-defined species. We also present experimental validation of CAFES using the data from well-controlled peak- and plateau-mode ITP processes.

PHYSICAL PROCESS AND MODEL DESCRIPTION

Advection−Diffusion Equations and Boundary Conditions. Assuming no bulk flow (e.g., pressure-driven or electroosmotic flows) and electromigration within a long straight channel with a uniform cross section, the mass conservation of weak electrolyte species is described by the following set of advection−diffusion equations

$$\frac{\partial c_i}{\partial t} = \frac{\partial}{\partial x}\left[\frac{\partial (D_i c_i)}{\partial x} - \mu_i E c_i\right],\ i = 1, 2, \ldots N \tag{1}$$

Here, c_i represents the analytical concentration of the i-th species family in a mixture of N species[11] and E is the local electric field. The first term on the right-hand side represents molecular diffusion, while the second corresponds to the electromigration of ionic species. The derivation leading to this equation includes writing the conservation equations (including diffusion, electromigration, and reaction) for an arbitrary species and then summing these over each species "family," defined as all of the ionization states of each molecule group. Hence, the source (creation and destruction) terms associated with acid−base dissociation reactions do not appear explicitly since the "species concentration" c_i represents the sum concentration across all ionization states.[11] The species family effective mobility and diffusivity are then respectively denoted as μ_i and D_i. As described by Bercovici,[11] a good estimate of the latter quantities (particularly mobility) is obtained by solving the chemical equilibrium of the total ion mixture at each point in space and time (see eq 19 in Bercovici et al.[11]). The set of all advection−diffusion equations for each species family is coupled through the local electric field E, which depends on the local conductivity field and thus all ionic species. For a constant applied current density, j, as simulated in CAFES, the local electric field is governed by the following equation (see eq 18 in Bercovici et al.[11]):

$$E = \frac{1}{\sigma}\left(j + \frac{\partial S}{\partial x}\right) \tag{2}$$

Here, σ is the local ionic conductivity (itself a function of local species concentrations and ionization states). The gradient involving S is associated with the ionic current carried by diffusion, and the variable S results from the proper summations over ionization states and families.[11]

Spatial Discretization. The governing equations are discretized in space using a finite volume method based on the symmetric limited positive (SLIP) scheme of Jameson.[16] The formulation of this scheme for simulating electrophoretic transport phenomena is described in detail by Bahga et al.[17] For simplicity, speed of computation, and to manage memory in the JavaScript implementation, we discretized the spatial domain $[0, L]$ with a uniform and stationary grid. (Note this is unlike SPRESSO, which uses an adaptive grid to resolve the high-gradient interfaces of such multispecies electrokinetic dynamics much more precisely.) The current finite volume-based SLIP scheme yields second-order spatial accuracy in the regions with a smooth solution and automatically switches to first-order accuracy in the regions with oscillations or local extrema. The SLIP method's unconditional numerical stability allows for fast and stable simulations performed with a minimal number of grid points immediately prior to performing more accurate (but longer) simulations. It also explicitly conserves the mass of ionic species.

It is often unnecessary to simulate the entire length of the microchannel, and we can instead simulate ITP in a small, relevant portion. It is thus necessary to impose nonreflecting boundary conditions to prevent spurious reflections of concentration gradients propagating out of the computational domain.[11] These conditions are enforced by extending the

https://doi.org/10.1021/acs.analchem.1c03925
Anal. Chem. 2021, 93, 15768−15774

Table 1. Overview Table of the Parameters, Features, Inputs, Outputs, and Limitations of CAFES

model descriptor	description	units	comment or reference
physical equations	multispecies 1D unsteady electromigration and diffusion		Bercovici[11]
spatial discretization	symmetric limited positive (SLIP) scheme		Jameson,[16] Bahga[17]
time-stepping	Runge−Kutta-Dormand−Prince (DorPri45, 5th-order)		Bercovici[11]
model restrictions	ODE tolerance (see below) minimum of 10^{-2} (see SI)		
	initial interface widths σ assumed to be 1 mm	mm	read-only value
	suggested pH range of 3−11		
maximum grid points	no limit due to the numerical implementation		maximum set by results export
boundary and initial conditions	user-specified initial loading (see species parameters)		Bercovici[25]
	nonreflective boundary conditions		Leveque[18] and Bercovici[25]
	current density evolution equations		eqs 35−44 of Bercovici[25]
implementation languages	simulation: JavaScript (TensorFlow), Python		
	UI: JavaScript, HTML, CSS		
	post-processing using Python		
input parameters	simulation time (physical duration to be simulated)	s	
	steps per plot update	steps	increase to plot less often
	ODE error tolerance		
	domain length	mm	
	applied current	μA	signed float
	channel cross-sectional area	μm^2	
	species parameters (see below)		
species parameters	species name		character string
	type: right/left plateau, peak/plateau or uniform distribution		type describes spatial distribution
	total species concentration, c_0 (for right/left plateaus and uniform)	mM	nonnegative float
	total moles of species (only for peak/plateau distribution)	pmol	nonnegative float
	injection location (required for peak/plateau and right/left plateau) x_{inj}	mm	nonnegative float
	injection width (required only for peak/plateau zone)	mm	nonnegative float
	species valence(s)		signed integer
	species mobility(ies) of respective valence(s) $\lvert\mu\rvert$	10^{-9} $m^2/(V{\cdot}s)$	nonnegative float
	pK_a(s) associated with valence transition	pH units	signed float
common species database	contains a total of 521 species: 303 weak acids, 161 weak bases, and 57 ampholytes. 179 species have multiple relevant valences.		Hirokawa[15]
	string search		
	direct integration of the database in the input (add button)		
alternate input	configuration file (contains all input parameters and species data, load config button)		JSON file
output	configuration file (save config button)		JSON file
	save results folder contains nonreadable spatial-temporal cube and inputs		ZIP file
	Analyze tool replays concentration plot dynamics directly in the UI (no post-process)		Plotly[19]
real-time line plot features (Analyze tool)	plotted are color-coded total (analytical) concentrations, pH and electric field vs distance	mM, pH units or V/mm vs mm	Plotly[19]
	species name in legend corresponds to input name		
	reset scale by clicking the home button		
	zoom in/out, pan, and autoscale features		
	isolate one profile by double-clicking on its legend	mM vs mm	
	plot shows simulated time	s	

computational domain on both ends using ghost cells in which the species concentrations are equal to the species concentrations at the corresponding boundary at every time step.[11,18]

Time Discretization. We adopted the fifth-order Runge−Kutta-Dormand−Prince (DorPri45) method for time integration. (This is the method used by, for example, the ode45 function in MATLAB, although we here use JavaScript.) It adjusts the time step at each iteration. The process of each time iteration is saved as a TensorFlow graph, which can be called upon by the JavaScript interface. The simulation sequence can be described as follows:

(1) User inputs the settings of the simulation and initiates the simulation.

(2) The domain is discretized in regular and constant spatial intervals.

(3) The TensorFlow graph object for the time iterations is generated based on the user-defined inputs and serialized.

(4) The governing equations for the species profiles are integrated using DorPri45 integration. At each iteration, the model generated in Step 3 is reloaded and infers the solution using the current adapted time step.

https://doi.org/10.1021/acs.analchem.1c03925
Anal. Chem. 2021, 93, 15768−15774

(5) Step 4 (and therefore Step 3) are repeated until the total time specified by the user is reached or if the user stops the simulation.

All computations are performed on the client's side, i.e., within the user's browser software. This means there is no need to download the results file through the Internet. The computed solution can, in all cases, be observed and interacted using the Plotly[19] user interface.

User Input and Output. CAFES takes as input the parameters summarized in the inputs section of Table 1. An example image of the input general user interface (GUI) panel is shown as Figure S1 of the Supporting Information (SI).

The user defines the channel cross-sectional area and total length of the channel of interest. The initial configuration of buffers and sample ions is then established as follows. First, the user selects each chemical species, either choosing from the database or by defining a custom species. Next, the user determines the initial distribution of the species and its physicochemical properties.

The chemical properties of interest are the valence(s), the fully ionized (i.e., absolute) mobility(ies), and the pK_a('s) of each species. The code includes a database[11,15] of 521 common chemical species, whose makeup is summarized in Table 1. The user can search through this database using the provided string-based search tool and automatically add the desired species with a click of an add "+" button. The user can also enter custom species and families of custom species (e.g., protonated and deprotonated forms of a weak acid), which can be specified using commas in the same input row. Lastly, the user sets the electric current to drive ITP. We assume only constant current mode for simplicity.

Each species can be introduced into the problem with one of four different initial spatial profiles. The "Left Plateau" and "Right Plateau" profiles are useful in the simulation of species, which begin at the respective left and right end of the domain, extend into the domain, and terminate somewhere within it. These distributions are prescribed by the initial species concentration (c_0), the injection location (x_{inj}) (i.e., the location where the species is terminated), and interface width (σ) associated with the interface as follows

$$c(x) = \frac{c_0}{2}\left[1 \pm \mathrm{erf}\left(2\frac{x - x_{inj}}{\sigma}\right)\right] \tag{3}$$

Next, the "Peak" distribution can be used to model a species injected into some finite space within the channel. This distribution is parametrized by the total injection amount (N) in moles, an injection location (x_{inj}), an injection width (w), interface width (σ), domain length (L), and cross-sectional area (A) following the equation

$$c(x) = \frac{N \cdot g(x)}{\int_0^L g(s) \cdot A \cdot \mathrm{d}s} \tag{4}$$

Here, $g(x)$ is defined as

$$g(x) = \mathrm{erf}\left(\frac{2}{\sigma}(x - x_{inj} + w)\right) - \mathrm{erf}\left(\frac{2}{\sigma}(x - x_{inj} - w)\right) \tag{5}$$

The characteristic injection width w can approach (and even be smaller than) the characteristic interface width. For $w < \sigma$ (which is a valid input to the simulation), the spatial profile approaches a Gaussian-like top hat distribution. Lastly, the "uniform" distribution can be used to simulate some background species injected with uniform fixed concentration throughout the whole domain length (and presumably outside of it so that the species can enter and leave the domain). This distribution is thus specified by only one parameter: the uniform initial concentration (c_0).

In the Simulation and Numerics section of the input panel, the user sets the number of grid points, the total simulation time, and the absolute ordinary differential equation integration tolerance (ODEIT). Lower ODEIT implies that the simulation is more accurate, and we recommend a value of less than about 10^{-2} for rough estimates and less than 10^{-4} for more accurate results (see SI for additional details on ODEIT). The whole input configuration can be saved and exported for future use as a JavaScript Object Notation (JSON) file.

The Start button initiates the simulation. The Plotly interface provides direct visualizations of all species concentrations, the pH and the electric field at the latest time iteration. This interface allows the user to interact with the plot in real time using the tools provided by Plotly. The user can manually (Zoom, Zoom in/out, and Pan buttons) or automatically (Autoscale button) adjust the zoom on a portion of the abscissa and/or ordinance of the simulation, toggle spike lines to easily read numerical values, isolate the plot of a single species (double click on the legend of the corresponding species), and reset the original view (via the Reset Axes button). At any time, the user is free to pause (or stop) the simulation and export the results as a ZIP folder containing multiple binary files. These files contain the input, the time steps, and the electrolyte concentration profiles (H^+ having a separated binary file), in addition to the electric field profile. This export is not directly readable, but we have provided Python tools to decode it and describe these in the SI. The concentration and pH profiles can be obtained for each time.

EXPERIMENTAL METHODS

We validated the computations of CAFES by comparing its predictions to the experimental data for both peak-and plateau-mode ITP. We compared the output of the simulation to two sets of experimental data. First is a set of data obtained as part of the current study (specifically to evaluate peak-mode dynamics). The second is a set of plateau-mode ITP data originally published by Chambers et al.[20] We describe these below.

We performed peak-mode focusing of Alexa Fluor (AF) 488 in a single, off-the-shelf borosilicate microfluidic chip (model NS12AZ, Caliper Life Sciences, subsidiary of PerkinElmer, Inc.). Figure S3 in the SI shows a schematic of the chip. It consists of two channels wet-etched to a 20 μm depth with a 50 μm mask width. This results in an approximately 1630 μm^2 D-shaped cross section. A constant but adjustable current (from 1 to 5 μA) was imposed between positive and negative electrodes separated by a total distance of 72 mm. The LE buffer consisted of 100 mM Tris and 50 mM HCl, and TE consisted of 100 mM Tris, 50 mM HEPES and 0.2 μM AF488. The initial buffer loading is detailed in Figure S3 of the SI. We monitored the progression of the peak using an inverted epifluorescence microscope with an objective with 4× magnification and NA of 0.2 (Nikon Plan Apochromat CFI60). We recorded all of the movies using a CMOS camera (Hamamatsu ORCA-Flash 4.0) at 20 fps (frames per second) and used a flat field correction to account for inhomogeneous illumination. The imaging results in a spatial, line-of-sight averaging of intensity along the depth of the channel. In post-process, we then averaged the fluorescence signal along the

https://doi.org/10.1021/acs.analchem.1c03925
Anal. Chem. 2021, 93, 15768−15774

spanwise width of the channel to isolate streamwise variations of dye concentration using a custom MATLAB code. Each averaged frame then constituted a single-point value versus time from which we constructed the spatial-temporal plot as shown in Figure 2A. For simplicity of presentation, the intensities of Figure 2A were normalized by the highest measured intensity across all experiments. This intensity maximum occurred near the end of the highest current condition, as expected.

The experimental setup for the plateau-mode data is detailed in Chambers et al.[20] and only summarized here. Chambers used a similar off-the-shelf glass microchip. Their LE buffer consisted of 100 mM MES, 200 mM BisTris, 2 mM $Ba(OH)_2$, and 0.4% PVP, and their TE buffer consisted of 100 mM tricine, 20 mM $Ba(OH)_2$, and 0.4% PVP. Variable concentrations of analytes (HEPES and MOPS) were added to the TE buffer in three different cases to observe different plateau lengths. AF488 was used as a nonfocusing tracer[20] in the plateau-mode ITP experiments.

RESULTS

ITP Simulations Using CAFES. The simulation tool outputs the concentration profiles of all species at each time instant. The different injection types ("Left plateau," "Right plateau," and "Peak") can be combined to construct a wide variety of complex initial concentration profiles.

To show the versatility of the tool, we simulated a simultaneous fairly complex anionic ITP process and showed four selected time instants of the simulation in Figure 1. In this example, the initial concentrations of three analytes result in two plateau-mode analytes (weak acids MES and MOPS) and one peak-mode analyte (fluorescent dye AF488). The initial LE mixture included a rapid reduction in concentration at x = 60 mm. This LE distribution is simulating a so-called cascade ITP,[21] wherein an initial high LE concentration is used to improve the sample ion capacity of the system and then transition to a higher electric field region which provides better plateau resolution. The dynamics show the development and motion of various ion interfaces and pH throughout the computational domain of interest. Note the two stationary "top hat" features in the HEPES distribution (centered near x = 20 and 40 mm) are stationary, expected, and due to the Jovin and Alberty regulating functions established by the initial distribution of ions.[22] We present additional examples of CAFES simulations for cationic and for bidirectional ITP in the SI (and provide example input files for these computations). In the next two sections, we will show experimental validation for the tool by comparing predictions to peak- and plateau-mode anionic ITP experimental data.

Peak-Mode Simulations and Comparison to Experiments. For peak-mode simulations, we followed the input protocol described above to match the conditions of the experiment. To this end, we simulated a total length of 32 mm segmented into 3000 uniform intervals. Theoretical diffusivities and absolute mobilities values of AF488 were reported in Milanova et al.[23] Taking advantage of the expected (and observed) proportionality between ITP velocity and current, we ran each simulation for a total time inversely proportional to the imposed current to match the final spatial position of the ITP peak in every simulation. We then post-processed the JSON output file to plot the concentration profile of AF488 at each time step and obtain spatial-temporal plots comparable to the ones resulting from the experimental data. Each spatial-temporal

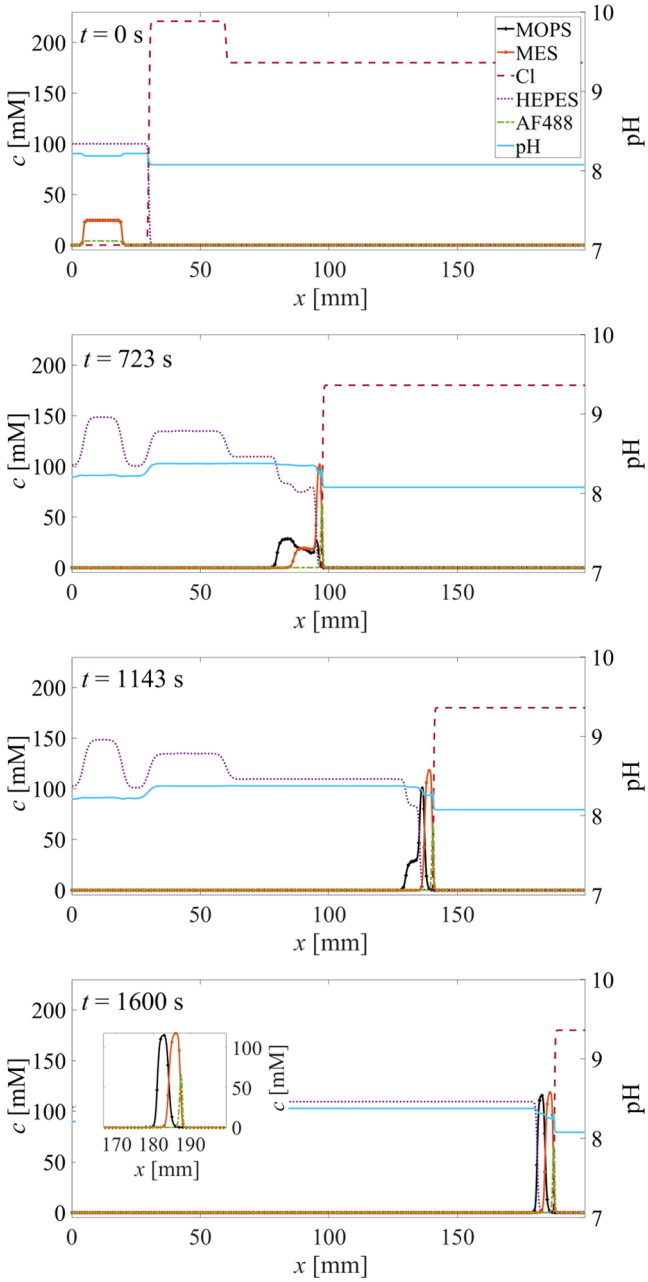

Figure 1. Simulation of anionic ITP process using CAFES. Plotted are concentration profiles of ions (left ordinate) and pH (right ordinate) at four time instants. Species are an LE anion (HCl), TE anion (HEPES), and three simulated analytes (MOPS, MES, and Alexa Fluor 488). TE buffer is 200 mM Tris and 100 mM HEPES (computed pH = 8.2). LE buffer is 440 mM Tris and 220 mM HCl for $x_i \in [30\text{ mm}, 60\text{ mm}]$ (at t = 0 s) and 360 mM Tris and 180 mM HCl for $x_i \in [60\text{ mm}, 200\text{ mm}]$. Initial amounts of MOPS, MES, and Alexa Fluor 488 are respectively 600, 600, and 100 pmol. The inset plot at t = 1600 s shows the detailed concentration profile of the three analytes. Two of these focus in plateau mode and a third in peak mode. This simulation was performed using 1000 grid points.

plot in Figure 2B was normalized by the corresponding integrated fluorescent signal in the experimental plot (Figure 2A).

As shown in Figure 2, the predicted peak-mode dynamics compare well to the experimental data. The predicted velocities (corresponding to slope values in the figure) for 1, 2, 3, and 5 μA respectively match within 7, 10, 11, and 5% of the measured

https://doi.org/10.1021/acs.analchem.1c03925
Anal. Chem. 2021, 93, 15768−15774

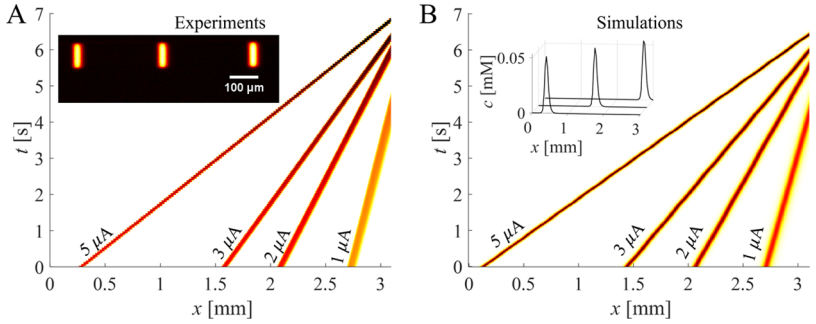

Figure 2. Comparison between experimental quantitative visualizations of a focused dye (A) and corresponding simulations (B) for peak-mode ITP. (A) Spatiotemporal plots of width-averaged fluorescent signal on the chip. Four spatiotemporal data traces are superposed in the main plot. The inset shows three experimental images of the same ITP peak at three different times for an applied current of $I = 5\ \mu$A. (B) Spatiotemporal plot of the focused species concentration as predicted by CAFES. Four simulated traces are superposed in the same figure. The inset shows the predicted concentration profiles at three different times for an applied current of $I = 5\ \mu$A. The simulations well capture propagation speed, accumulation rate, and the trends in peak width, with higher currents, resulting in proportionally narrower widths.

values. In all cases, the observed velocity was slightly higher than the prediction, and this may be due to a bias error in the estimate of the channels' cross-sectional area. Further, the simulations well capture the trend in peak width, with the highest current resulting in the thinnest peak as expected. The simulations also capture the finite rate of accumulation of analyte observed in the semi-infinite ITP injection. This is most apparent in the plot for the data at 5 μA, where we observe a 1.25 concentration fold-increase within the observation frame in the simulation, compared to 1.22 in the corresponding experiment. Lastly, note that the experimentally observed straight and perpendicular (to channel axis) shape of the ITP zone (see inset images in Figure 2A) is consistent with an experiment with very low dispersive effects (e.g., from residual electroosmotic flow or mismatched reservoir liquid heights).

Plateau-Mode Simulations and Comparison to Experiments. We set up the plateau-mode simulations to match the experimental conditions of Figure 4 of Chambers et al.[20] The simulation domain was 50 mm long and divided into 1500 intervals. Our simulations included all of the chemistry specifications of the Chambers experiments, including AF488 dye (modeled[23] using a fully ionized mobility of 36×10^{-9} m^2/(V·s) and pK_a of −2). After performing the simulations, we used the Python post-processing tools to plot the concentration profile of AF488 using an intensity color scale similar to that of the experimental data.

Simulations and experiments are both shown and compared in Figure 3. The AF488 dye fluorescence intensity distribution is expected to be proportional to the local electric field and consistent with simulations. In particular, the fluorescence intensity varies rapidly within each plateau-to-plateau interface, and so this intensity distribution is useful in quantifying plateau width and location. From left to right, the observable plateaus are the TE, HEPES, MOPS, and LE. We note that the CAFES predictions of plateau widths and locations match very well with the experimental data. The relative intensities among plateaus also compare well between simulations and experiments. Note the simulation captures the observed variations in plateau width associated with the variations in the initial focused amount of each species in these finite-injection ITP experiments. The differences between model predictions and the quantitative measurements of ion concentration of the various plateau regions differ by less than about 6%. We attribute this to various experimental uncertainties, including minor irreproducibility in background signals and the dependence of the dye quantum

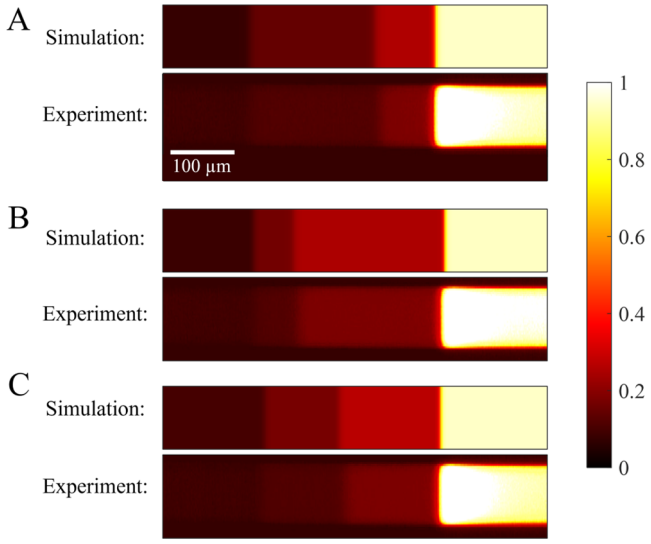

Figure 3. Detection of analyte plateaus with a fluorescent nonfocusing tracer (NFT) (second, fourth, and sixth images, starting from the top) and corresponding simulations (first, third, and fifth images). For each experimental condition, the top panel shows a fluorescent on-chip experimental[20] signal. The plateaus correspond to, from left to right, TE, HEPES, MOPS, and LE. The concentrations of the HEPES and MOPS (injected as a finite sample zone) were respectively 9 and 3 mM (A), 3 and 9 mM (B), or 6 mM each (C). The bottom panels show the corresponding predictions from CAFES: the NFT concentration profile is plotted using a color scale similar to that of the experimental figure. All three simulations show good estimates of plateau lengths and relative intensities.

yield on ionic strength and pH. Note also that the current simulations do not include ionic strength effects. Bahga et al.[12] describe quantitative experiments and comparison with ITP models that include the effect of ionic strength on ion mobilities and on weak electrolyte (acid) dissociation constants (i.e., pK_a values). The largest discrepancy between simulations and experimental visualizations is around the significant overshoot of fluorescence intensity observed by Chambers et al.[20] near the left edge of the LE. In the experiment, the fluorescence intensity rises sharply as you travel from left to right through the MOPS-to-LE interface (as expected) but then overshoots the expected intensity within the LE before settling down to the expected locally uniform value for the LE. This type of overshoot is commonly observed in such NFT experiments (e.g., Bahga et

https://doi.org/10.1021/acs.analchem.1c03925
Anal. Chem. 2021, 93, 15768−15774

al.[24]). Interestingly, the physical reason for this overshoot is not well understood and currently not captured by ITP simulations. We hypothesize this overshoot may be due to trace fluorescent impurities in the system (e.g., perhaps degraded or complexed forms of the dye itself) that focus in peak-mode at the left edge of the LE zone.

CONCLUSIONS

We demonstrated implementation and experimental validation of CAFES, a web-based simulator for nonlinear and complex electrophoresis problems, including ITP. This highly interactive tool provides quick estimations of ITP dynamics of weak electrolytes using the SLIP scheme and Dormand−Prince 45 integration and benefits from the broad compatibility of JavaScript and its operation on client-side browser software. CAFES provides a platform that can be used to design and evaluate ITP experiments, including parameters such as spatiotemporal concentration fields of all species and of pH, interface velocities, electric field profile, and plateau lengths. For simplicity and to decrease the computational time, the code uses a uniform grid, which captures these parameters accurately but then only very approximately captures the spatial extent of the sharp gradients associated with plateau-to-plateau interfaces. We validated the simulations using experimental data from both peak-and plateau-mode experiments. CAFES was able to well capture propagation velocities, accumulation rates, plateau order, plateau widths, and plateau intensities. It is currently available for free at https://microfluidics.stanford.edu/cafes and requires no license nor compilation.

ASSOCIATED CONTENT

Supporting Information

The Supporting Information is available free of charge at https://pubs.acs.org/doi/10.1021/acs.analchem.1c03925.

> Additional information and details about experimental methods and simulation settings; screenshots of the general user interface of the tool, post-processing and export procedures, microfluidic chip geometry and initial injection profile, additional ITP simulation examples, and a grid independence study (PDF)

AUTHOR INFORMATION

Corresponding Author

Juan G. Santiago − *Department of Mechanical Engineering, Stanford University, Stanford, California 94305, United States;* orcid.org/0000-0001-8652-5411; Email: juan.santiago@stanford.edu

Authors

Alexandre S. Avaro − *Department of Mechanical Engineering, Stanford University, Stanford, California 94305, United States;* orcid.org/0000-0003-1922-3629

Yixiao Sun − *Department of Mechanical Engineering, Stanford University, Stanford, California 94305, United States*

Kaiying Jiang − *Department of Mechanical Engineering, Stanford University, Stanford, California 94305, United States*

Supreet S. Bahga − *Department of Mechanical Engineering, IIT Delhi Hauz Khas, New Delhi 110016, India*

Complete contact information is available at: https://pubs.acs.org/10.1021/acs.analchem.1c03925

Notes

The authors declare no competing financial interest.

ACKNOWLEDGMENTS

The authors gratefully acknowledge funding from Stanford University's Interdisciplinary Biosciences Institute (Bio-X) and from Stanford's School of Engineering COVID-19 Research and Assistance Fund.

REFERENCES

(1) Khurana, T. K.; Santiago, J. G. *Anal. Chem.* **2008**, *80*, 6300−6307.
(2) Garcia-Schwarz, G.; Rogacs, A.; Bahga, S. S.; Santiago, J. G. *J. Visualized Exp.* **2012**, *61*, No. e3890.
(3) Everaerts, F. M.; Beckers, J. L.; Verheggen, T. P. E. M. *Isotachophoresis: Theory, Instrumentation and Applications*, 1976; Elsevier Scientific Publishing Company.
(4) Rogacs, A.; Marshall, L. A.; Santiago, J. G. *J. Chromatogr. A* **2014**, *1335*, 105−120.
(5) Bahga, S. S.; Santiago, J. G. *Analyst* **2013**, *138*, 735−754.
(6) Eid, C.; Santiago, J. G. *Lab Chip* **2018**, *18*, 11−26.
(7) Khnouf, R.; Han, C. *IEEE Nanotechnol. Mag.* **2020**, *14*, 6−17.
(8) Ramachandran, A.; Huyke, D. A.; Sharma, E.; Sahoo, M. K.; Huang, C.; Banaei, N.; Pinsky, B. A.; Santiago, J. G. *Proc. Natl. Acad. Sci. U.S.A.* **2020**, *117*, 29518−29525.
(9) Schwer, C.; Gaš, B.; Lottspeich, F.; Kenndler, E. *Anal. Chem.* **1993**, *65*, 2108−2115.
(10) Gaš, B.; Bravenec, P. *Electrophoresis* **2021**, *42*, 1291−1299.
(11) Bercovici, M.; Lele, S. K.; Santiago, J. G. *J. Chromatogr. A* **2009**, *1216*, 1008−1018.
(12) Bahga, S. S.; Bercovici, M.; Santiago, J. G. *Electrophoresis* **2010**, *31*, 910−919.
(13) Dagan, O.; Bercovici, M. In*Novel Simulation Tool Coupling Nonlinear Electrophoresis and Reaction Kinetics*, Proceedings of The Sixteenth International Conference on Miniaturized Systems for Chemistry and Life Sciences (μTAS 2012), 2012.
(14) Garcia-Schwarz, G.; Bercovici, M.; Marshal, L.; Santiago, J. G. *J. Fluid Mech.* **2011**, *679*, 455−475.
(15) Hirokawa, T.; Kiso, Y. *J. Chromatogr. A* **1982**, *252*, 33−48.
(16) Jameson, A. *Int. J. Comput. Fluid Dyn.* **1995**, *4*, 171−218.
(17) Bahga, S. S.; Bercovici, M.; Santiago, J. G. *Electrophoresis* **2012**, *33*, 3036−3051.
(18) Leveque, R. J. *Finite-Volume Methods for Hyperbolic Problems*; Cambridge University Press, 2002.
(19) Plotly JavaScript Open Source Graphing Library. https://plotly.com/javascript/ (accessed Oct 19, 2021).
(20) Chambers, R. D.; Santiago, J. G. *Anal. Chem.* **2009**, *81*, 3022−3028.
(21) Boček, P.; Deml, M.; Janak, J. *J. Chromatogr. A* **1978**, *156*, 323−326.
(22) Ramachandran, A.; Santiago, J. G. *Microfluidic Isotachophoresis: Theory and Applications*. 2021, arXiv:2108.09595. arXiv.org e-Print archive. https://arxiv.org/abs/2108.09595.
(23) Milanova, D.; Chambers, R. D.; Bahga, S. S.; Santiago, J. G. *Electrophoresis.* **2011**, *32*, 3286−3294.
(24) Bahga, S. S.; Santiago, J. G. *Electrophoresis.* **2012**, *33*, 1048−1059.
(25) Bercovici, M.; Lele, S. K.; Santiago, J. G. *J. Chromatogr. A* **2010**, *1217*, 588−599.